

Tuhina Banerjee

Nand Kishore

Department of Chemistry,
Indian Institute of Technology,
Bombay, Powai,
Mumbai—400 076, India

Does the Anesthetic 2,2,2-Trifluoroethanol Interact with Bovine Serum Albumin by Direct Binding or by Solvent-Mediated Effects? A Calorimetric and Spectroscopic Investigation

Received 20 January 2005;

accepted 15 February 2005

Published online 28 February 2005 in Wiley InterScience (www.interscience.wiley.com). DOI 10.1002/bip.20262

Abstract: Thermal unfolding of bovine serum albumin (BSA) has been studied in the presence of 2,2,2-trifluoroethanol (TFE) using high-sensitivity microdifferential scanning calorimetry. Quantitative thermodynamic parameters accompanying the thermal transitions have been evaluated. TFE is observed to be a stabilizer or a destabilizer of the folded state of BSA depending on the pH. CD spectroscopy revealed an increase in the α -helical content of BSA and a decrease in the tertiary structure in the presence of increasing molalities of TFE. Isothermal titration calorimetric results do not indicate appreciable binding of the TFE molecules to BSA. TFE quenches the steady-state tryptophan fluorescence of BSA only at higher molalities and there is no effect on the tryptophan fluorescence at lower molalities. The calorimetric and spectroscopic results obtained in this work suggest that solvent-mediated effects dominate the interaction of TFE with BSA and the binding component may be very weak. Since the binding component is very weak, one of the possibilities of anesthetic action of TFE molecules on the actual targets may be through perturbation of the structural and dynamic properties of the lipid bilayer so that the function of crucial but unspecified membrane proteins is affected. © 2005 Wiley Periodicals, Inc. *Biopolymers* 78: 78–86, 2005

This article was originally published online as an accepted preprint. The "Published Online" date corresponds to the preprint version. You can request a copy of the preprint by emailing the *Biopolymers* editorial office at biopolymers@wiley.com

Keywords: bovine serum albumin; 2,2,2-trifluoroethanol; differential scanning calorimetry; isothermal titration calorimetry; spectroscopy

INTRODUCTION

An understanding of the protein–solvent interactions is essential to elucidate the nature of forces that stabilize the native conformation of proteins under a given solvent environment. The effect of alcohols on proteins and peptides is useful for considering how protein-

specific structures are stabilized in an aqueous environment.¹ Such studies provide insights into biologically important events as alcohols modify the folding pathway of proteins,^{2,3} mimic the environment of biomembranes,⁴ and induce assembly of biologically relevant peptides.⁵ Due to mixed hydrophilic–hydrophobic character, alcohols, especially those fluorosubstituted, have

Correspondence to: Nand Kishore; email: nandk@chem.itb.ac.in
Contract grant sponsor: Department of Science and Technology, New Delhi, India.

This article includes Supplementary Material available from the authors upon request or via the Internet at <http://www.interscience.wiley.com/jpages/0006-3525/suppmat>.

Biopolymers, Vol. 78, 78–86 (2005)

© 2005 Wiley Periodicals, Inc.

been widely used to generate partially folded states in proteins and peptide fragments.^{6–13} Alcohols are known to denature the native state of proteins by weakening the hydrophobic interactions. They also stabilize the α -helical conformation in proteins by minimizing the exposure of peptide backbone.^{14–18} Apart from an understanding of the protein-folding problem, alcohol–protein interactions are also important in a wide range of applications such as dissolution of aggregates that occur during peptide synthesis, investigation of prion diseases, and Alzheimer’s amyloid peptides.^{19,20}

2,2,2-Trifluoroethanol (TFE) is extensively used amongst the fluorosubstituted alcohols to generate the partially folded states.^{7–9,18,21} TFE has been found to stabilize helical structures, β -sheets, and β -hairpins.^{22–24} The mechanism proposed for the helix-inducing ability of TFE has been proposed to be either by helix stabilization or by direct binding of TFE to the peptides or through solvent-mediated effects.^{25–27} However, direct binding proposal of the TFE to proteins still requires experimental proof. TFE has also been reported to exhibit anesthetic properties.²⁸ It is a metabolite of anesthetic agents and chlorofluorocarbon alternatives.²⁹ The most commonly used measure of volatile anesthetic potency *in vivo* is the minimum alveolar concentration (MAC), and $C_{\text{anesthetic}}$ is an average of these MAC values, which is $24.3 \times 10^{-3} \text{ mol dm}^{-3}$ for TFE in mammals.²⁸ To understand the physicochemical basis of the anesthetic potency of TFE, we have chosen bovine serum albumin (BSA) as the model protein. Serum albumins are the best-studied models for general anesthetic binding because of their abundance and properties. They contain a number of cavities that bind a wide array of amphipathic hormones, metabolites, and pharmaceuticals.^{30–32} In view of the anesthetic and secondary structure stabilizing properties of TFE, we have studied the thermal unfolding and conformational changes of BSA in the presence of TFE, and the mode of interaction of the alcohol with the protein, quantitatively using a combination of differential scanning calorimetric, isothermal titration calorimetric, CD, and fluorescence measurements. Such studies can provide guidelines for plausible explanation of the mechanism of action of TFE with the proteins present in the central nervous system, which are the actual targets where the anesthetics bind.

MATERIALS AND METHODS

Materials

BSA and TFE of the best available purity grade were purchased from Sigma-Aldrich Chemical Company USA and

used without further purification. The BSA used was lyophilized powder, and the purity and fatty acid content as listed by the vendor are ≥ 96 and 0.005% respectively. The mass fraction purity of TFE checked by gas chromatography was 0.99. A Sartorius BP 211D digital balance of readability $\pm 0.01 \text{ mg}$ was used for the mass measurements. The water used for preparing the solutions was double distilled and then deionized using a Cole-Parmer research mixed-bed ion exchange column. The protein was dialyzed extensively against $20 \times 10^{-3} \text{ mol dm}^{-3}$ potassium phosphate at pH 7.0 and $20 \times 10^{-3} \text{ mol dm}^{-3}$ glycine–NaOH at pH 9.0 with at least four changes of the respective buffer at 277.15 K. The reported pH is that of the dialysate measured on a Standard Control Dynamics pH meter at room temperature. The concentration of BSA was determined spectrophotometrically on a Shimadzu double beam spectrophotometer UV 265 at 280 nm using $A^{1\%, 1\text{cm}} = 6.8$.³³

Differential Scanning Calorimetry

The thermal denaturation experiments were performed on SETARAM micro differential scanning calorimeter (DSC) equipped with removable Hastelloy C-276 fluid tight batch cells of 1-cm^3 capacity. Before loading into the calorimetric cells, all the solutions were degassed. Any loss in water thus evaporated, determined from the mass of the sample before and after degassing, was compensated by addition of an appropriate amount of degassed deionized water. The volume of the sample solution in the cell was fixed at 0.85 cm^3 and the weights of the sample and reference cells containing respective solutions were always matched to within 0.1 mg. An excess power vs. temperature scan for the protein transitions was obtained by subtracting the power input of thermal scan of solvent in both the cells from the power input scan of the protein solution in the sample cell and solvent in the reference cell. The excess power thermal scans were also corrected for the thermal lag of the calorimeter and then converted to excess heat capacity vs. temperature scan by dividing by the scan rate. The corrected DSC data were analyzed by the EXAM program of Kirchoff.³⁴ The calorimetric reversibility of the thermal transitions was determined by heating the sample to a temperature that is a little above the transition maximum, cooling immediately, and then reheating.

Isothermal Titration Calorimetry

Isothermal titration calorimetry (ITC) measurements were carried out at 25°C on a VP- ITC titration calorimeter (Micro Cal, Northampton, MA). Before loading, the solutions were thoroughly degassed by using Thermo Vac supplied by MicroCal, LLC, USA. The reference cell was filled with the respective degassed buffer. The protein was kept in the sample cell and aqueous TFE was filled in the syringe of volume 250 μL . The alcohol solution was added sequentially in 10- μL aliquots (for a total of 25 injections, 20-s duration each) at 4-min intervals. The heat of dilutions were determined with similar parameters by injecting (i) by injecting $8.34 \times 10^{-3} \text{ mol kg}^{-1}$ TFE solution in buffer at

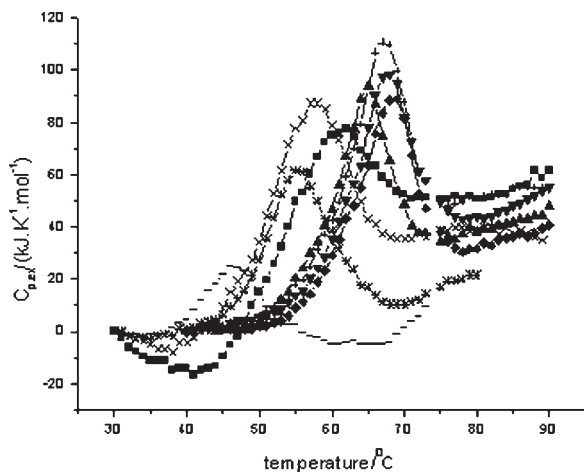


FIGURE 1 Thermal transitions of $0.12 \times 10^{-3} \text{ mol dm}^{-3}$ BSA at pH 7 in the presence of varying molalities of TFE: 0 (■), 0.1 (●), 0.25 (▲), 0.50 (▼), 0.75 (◆), 1.0 (+), 2.0 (×), 2.5 (*), and 3.0 (–) mol kg^{-1} .

respective pH, (ii) by injecting buffer solution into $0.058 \times 10^{-3} \text{ mol dm}^{-3}$ BSA, and (iii) buffer into buffer solution. The respective heats of dilution were subtracted from the corresponding BSA–TFE profiles prior to curve fitting. Calorimetric data were analyzed using Micro Cal Origin software supplied with the instrument. The enthalpy change for each injection was calculated by integrating the area under the peaks of recorded time course of change of power.

CD Experiments

The CD experiments were performed on a Jasco-810 CD spectropolarimeter at 25°C . The protein concentration and path length of the cell used were $10 \mu\text{M}$ and 0.1 cm for far-UV CD and $30 \mu\text{M}$ and 1 cm for near-UV CD respectively. The spectropolarimeter was purged with nitrogen gas prior to the experiment. Each CD plot was an average of three accumulated plots, which were baseline corrected. The maximum error in the ellipticity measurements was 1%. The molar ellipticity was calculated from the observed ellipticity θ as $100 \cdot \theta/c \cdot l$, where c is the concentration of the protein solution in mol dm^{-3} and l is the path length of the cell in centimeters.

Fluorescence Experiments

The fluorescence experiments were performed at 25°C using the Perkin-Elmer LS-55 spectrofluorimeter. The protein concentration in all the experiments was kept at $0.5 \mu\text{M}$. The excitation and emission slit widths were fixed at 5 nm . The excitation wavelength was kept at 295 nm to selectively excite the tryptophan residues and emission spectra were recorded. All the fluorescence experiments were repeated at least thrice. The maximum error in the intensity measurements was within 1% and that in the wavelength maxima was less than 0.5 nm in the repeated experiments.

RESULTS AND DISCUSSION

DSC of BSA in the Presence of TFE

The representative DSC profiles of thermal denaturation of BSA in the absence and the presence of varying molalities of TFE at pH 7.0 are shown in Figure 1, and the corresponding thermodynamic parameters accompanying the thermal transitions are presented in Table I. Each value in this table represents an average of three experiments.

All the thermal scans consist of a single endothermic peak. The values of $T_{1/2} = 335.0 \text{ K}$ and $\Delta H_{\text{cal}} = 796 \text{ kJ mol}^{-1}$ of BSA at pH 7 are in good agreement with those reported in literature.³⁵ With an increase in the TFE molality from 0.1 to 1.0 mol kg^{-1} , the values of transition temperature and calorimetric enthalpy increased progressively up to 0.50 mol kg^{-1} , beyond which both properties showed a decrease. All the calorimetric transitions were observed to be partially reversible, restricting the application of equilibrium thermodynamics to evaluate the ratio of van't Hoff to calorimetric enthalpy.

The values of transition temperature and enthalpy of denaturation of BSA at pH 9 were found to be less than at pH 7 in the absence of alcohol, indicating that BSA is in a relatively more compact state at the physiological pH. The temperature dependencies of the excess heat capacity of BSA in the absence and in the presence of different molalities of TFE are shown in Figure 2. The corresponding thermodynamic parameters obtained via analysis of several DSC denaturation curves are given Table II.

Table I Thermodynamic Parameters^a Accompanying the Thermal Unfolding of $0.12 \times 10^{-3} \text{ mol dm}^{-3}$ BSA at pH 7 in the Presence of TFE at a Scan Rate of 0.5 K min^{-1}

TFE (mol kg^{-1})	$T_{1/2}$ (K)	ΔH_{cal} (kJ mol^{-1})
0.00	335.0	796
0.10	334.9	634
0.25	337.1	653
0.50	340.9	677
0.75	340.2	665
1.0	338.9	636
2.0	330.5	599
2.5	330.4	561
3.0	321.5	505

^a Incorporating errors in sample preparation, reproducibility, and sample impurities, the errors in the values of $T_{1/2}$ and ΔH_{cal} are $\pm 0.1 \text{ K}$ and 2% , respectively.

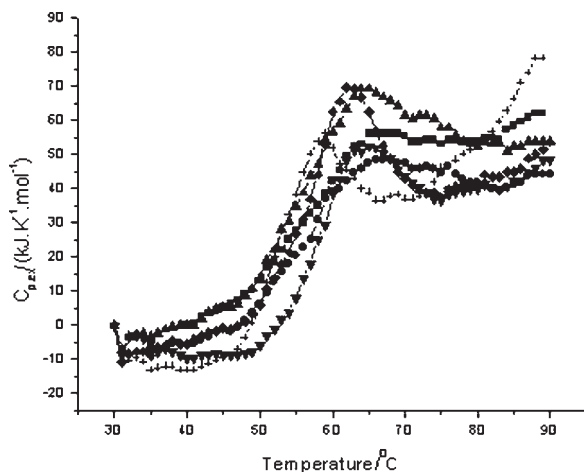


FIGURE 2 Thermal scans of 0.12×10^{-3} BSA at pH 9.0 in the presence of varying molalities of TFE: 0 (■), 0.1 (●), 0.25 (▲), 0.50 (▼), 1.0 (◆), 1.5 (+), 2.0 (×), and 3.0 (*) mol kg^{-1} .

Analysis of the Thermal Unfolding of BSA in the Presence of TFE at pH 7 and pH 9

Thermal denaturation of BSA in the presence of TFE can be explained on the basis of competing patterns of interactions of the cosolute with the native vs. unfolded state of the protein during the native \rightleftharpoons denatured reaction. It has been reported that the anesthetics like methanol, ethanol, propanol, halothane, and chloroform lower the transition temperature of proteins like chymotrypsinogen A,³⁶ ribonuclease,³⁷ and firefly luciferase.³⁸ However, we observed a slight increase in the value of transition temperature up to 0.5 mol kg^{-1} TFE in solution. The enhancement in the thermal stability of BSA at pH 7 upon addition of TFE unto 0.50 mol kg^{-1} could be due to (i) preferential interaction of cosolute/cosolvent with the native state of the protein compared to that with the denatured state, or (ii) alteration in the secondary or tertiary structural content of the protein under these conditions. Beyond 0.75 mol kg^{-1} both the values of transition temperature and calorimetric enthalpy decrease with the increase in the molality of the alcohol. This can be assigned to the stronger interaction of the TFE molecules with the denatured state of the protein compared to the native state under these conditions. At pH 9, the value of transition temperature decreased at all the studied molalities of TFE whereas the enthalpy of unfolding increased unto 1.50 mol kg^{-1} followed by a decrease.

CD of BSA in the Presence of TFE

To check whether the initial increase in the stability of BSA was accompanied by conformational

changes, CD experiments were carried out at pH 7.0, at all the molalities of TFE used in the calorimetric experiments. The far- and near-UV CD plots at different molalities of TFE at pH 7.0 are shown in Figure 3. It can be seen that BSA has a negative band near 208 nm and a relatively flat region of negative ellipticity between 210 and 225 nm. In the presence of TFE, the α -helicity increases in strength as reflected by the increased negative intensity of the band near 208 nm unto 0.75 mol kg^{-1} TFE, beyond which there is decrease in the α -helical content. The near-UV CD spectra of BSA indicate that there is a little perturbation in the wavelength zone between 260 and 280 nm of the chromophores of protein in the presence of the studied molalities of TFE. Even 3 mol kg^{-1} TFE did not produce any significant modification in the near-UV CD spectrum of the protein.

Enhancement of secondary structural content upon addition of fluoroalcohols has also been demonstrated in large number of peptides and proteins.⁶⁻¹³ The structure stabilizing property of fluoroalcohols has been proposed to arise from two important characteristics, namely, the hydrophobicity of the fluoroalkyl groups and the strong hydrogen-bond-donating/poor hydrogen-bond-accepting property of the hydroxyl groups.³⁹ Clustering of alcohol molecules is also an important factor that enhances the effect of alcohols on proteins and peptides.⁴⁰ Helicogenic effect exhibited by halogenated alcohols have been suggested to be a combination of a relatively low dielectric constant and a high dipole moment, the latter causing disruption of the internal hydrogen-bond networks and the former causing refolding to a helical configuration.³⁹

The far- and near-UV CD plots for BSA in the presence of TFE at pH 9.0, are shown in Figure 4 and

Table II Thermodynamic Parameters^a Accompanying the Thermal Unfolding of $0.12 \times 10^{-3} \text{ mol dm}^{-3}$ BSA at pH 9 in the Presence of TFE at a Scan Rate of 0.5 K min^{-1}

TFE (mol dm^{-3})	$T_{1/2}$ (K)	ΔH_{cal} (kJ mol^{-1})
0	336	426
0.10	335	547
0.25	334	572
0.50	334	657
1.00	332	698
1.50	330	741
2.00	326	591
3.00	318	494

^a Incorporating errors in sample preparation, reproducibility, and sample impurities, the errors in the values of $T_{1/2}$ and ΔH_{cal} are $\pm 0.1 \text{ K}$ and 2%, respectively.

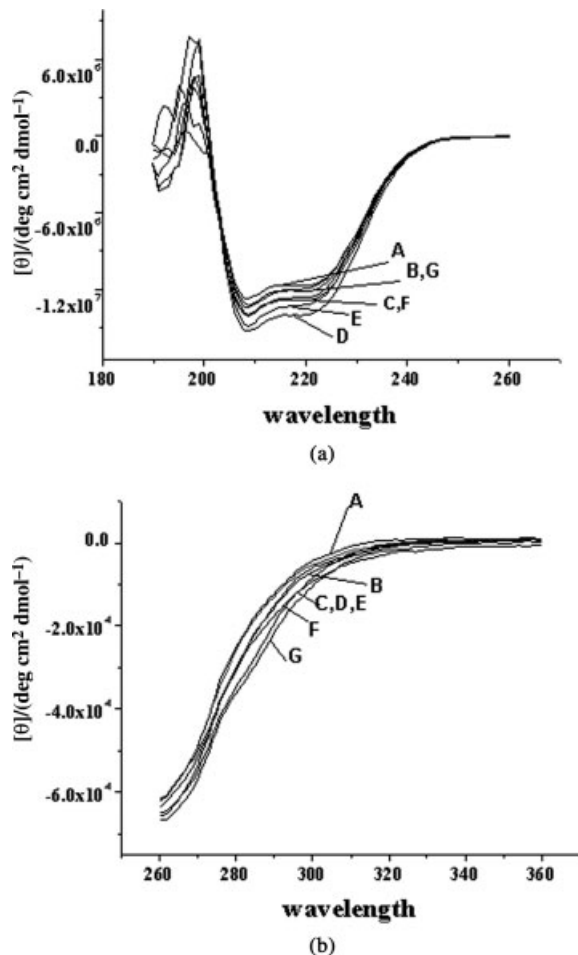


FIGURE 3 Far-UV CD spectra (A) and near-UV CD spectra (B) of BSA at pH 7 and at different molalities of TFE: 0 (A), 0.1 (B), 0.5 (C), 0.75 (D), 1.0 (E), 2.0 (F), and 3 (G) mol kg⁻¹.

supplement 1. There is an increase in the α -helicity at all the studied molalities of TFE. The tertiary structural content decreases with an increase in molality of TFE, which may be one of the reasons for the decrease in the thermal stability of BSA upon addition of TFE.

Figure 5 compares the change in transition temperature, enthalpy, molar ellipticity at 222 nm, and molar ellipticity at 260 nm for the interaction of BSA with TFE at pH 7 compared to these parameters in the absence of alcohol. All four different properties are found to vary along the same direction. A similar trend was also observed at pH 9.

Fluorescence of BSA in the Presence of TFE

Figure 6 presents the intrinsic fluorescence of BSA in presence of TFE at pH 7.0. It is observed that the

emission intensity decreases with an increase in the molality of TFE in solution. The values of wavelength maximum remains nearly the same from 0.05 to 1.5 mol kg⁻¹ TFE; a slight blue shift of 2 nm at 3 mol kg⁻¹ TFE suggests that as the molality of TFE is increased the tryptophan experiences more hydrophobic environment.

The extent of fluorescence quenching Q can be expressed as

$$Q = (F_0 - F/F_0) \quad (1)$$

where F_0 and F are the fluorescence intensities in the absence and the presence of quencher and Q_{\max} is the maximum quenched fluorescence. It follows from the mass law considerations that

$$Q = (Q_{\max} \cdot [\text{TFE}]/K_D + [\text{TFE}]) \quad (2)$$

where K_D is the average dissociation constant.

Figure 7 shows plot of fluorescence quenching of BSA vs. molality TFE at pH 7. Using a best-fit curve derived from Eq. (2), $Q_{\max} = 0.74 \pm 0.05$ and $K_D = 1.3 \pm 0.2$ mol kg⁻¹.

It has been reported that different halogenated alkanes and alcohols can effectively quench the tryptophan fluorescence of BSA at much lower concentrations.^{41,42}

Therefore, fluorescence experiments were also done at lower molalities of the alcohol ranging from 0.001 to 0.1 mol kg⁻¹. In this lower molality range, TFE did not quench the tryptophan fluorescence of BSA. These results indicate that TFE is effective in quenching the tryptophan fluorescence only at molalities higher than 0.1 mol kg⁻¹. A relatively lesser degree of quenching at lower molalities indicates that

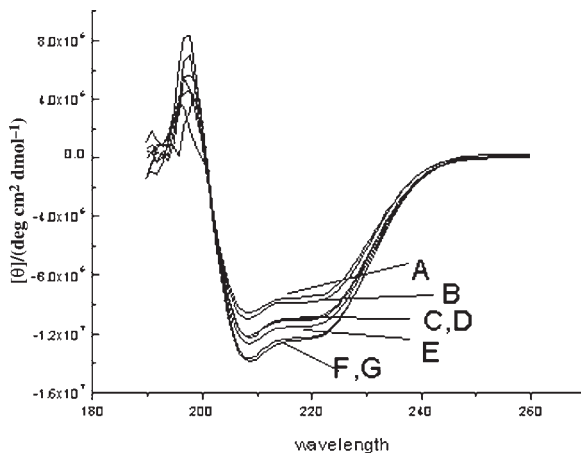


FIGURE 4 Far-UV CD spectra of BSA at different molalities of TFE at pH 9: 0.1 (A), 0.5 (B), 1.0 (C), 1.5 (D), 2.0 (E), and 3.0 (F) mol kg⁻¹.

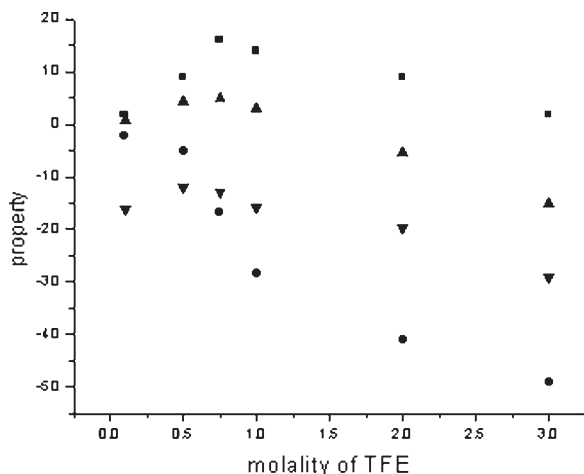


FIGURE 5 Plot of change in transition temperature/ $^{\circ}\text{C}$ (▲), molar ellipticity at 222 nm/deg $\text{cm}^2 \text{dmol}^{-1}$ (■), molar ellipticity at 260 nm/deg $\text{cm}^2 \text{dmol}^{-3}$ (●), and enthalpy/ kJ mol^{-3} (▼), compared to that in the absence of TFE.

TFE does not interact significantly with the protein matrix. The quenching at higher molalities of TFE may be attributed to high local concentrations of TFE in the immediate vicinity of the indole ring due to hydrophobic interactions between the TFE and the protein.

The emission spectra of BSA at pH 9 were characterized by well-resolved peaks. There is slight red shift of λ_{max} from 344 nm at pH 7 to 347 nm at pH 9 in the absence of alcohol. TFE causes a molality dependent decrease in the native tryptophan fluorescence of BSA, with a slight blue shift of 2 nm in the presence of 3 mol kg^{-1} TFE at both the pH values.

Using a best-fit curve derived from Eq. (2), the values of $Q_{\text{max}} = 0.46 \pm 0.05$ and the $K_{\text{D}} = 0.7 \pm 0.2 \text{ mol kg}^{-1}$ at pH 9 are obtained. Comparison of the Q_{max} at two different pH values suggest that TFE is more effective in quenching the fluorescence of BSA at pH 7. CD studies also show that in the presence of increasing molalities of TFE, the decrease in the tertiary structure is more at pH 9 whereas at pH 7 there is only a slight change in the tertiary structure. The diminished quenching of BSA at pH 9 suggests that tertiary structural elements are crucial for the interaction of TFE with the protein.

Isothermal Titration Calorimetric Data Analysis

Figure 8 shows the ITC profile for the titration of TFE with BSA at pH 7. The negative deviation from the stable baseline upon addition of TFE was very

small, toward the negative side, indicating that the process is slightly exothermic. The enthalpy change associated with each 10- μL injection of TFE plotted against the TFE to BSA molar ratio is shown in panel B of Figure 8. No variation in the heat evolved with the increase in the molar ratio was observed. Hence, the average of heat evolved at each injection was taken as the enthalpy of interaction.

The enthalpies of interaction of TFE with BSA at pH 7 and pH 9 are -4.45 ± 2.4 and $1.49 \pm 4 \text{ cal mol}^{-1}$ respectively. These values are nearly zero within the experimental uncertainty. The results do not indicate appreciable binding of TFE to BSA, thereby suggesting involvement of solvent-mediated effects due to changes in the structure of water induced by the cosolute in these interactions.

ITC results further support the fluorescence results where at lower molalities no quenching was observed; only at much higher molalities was partial quenching observed. Low values of K_{D} obtained from fluorescence results also indicate an absence of appreciable binding; therefore, the quenching at higher molalities can be attributed to solvent-mediated effects.

Mode of Interaction of TFE with BSA

The mechanism whereby TFE and other fluorinated alcohols induce protein structural changes still requires an experimental proof. Studies of interaction of TFE with short elastin peptide GVG(VPGVG) $_3^{43}$ suggest that TFE clusters locally assist the folding of secondary structures by first breaking down the interfacial water molecules on

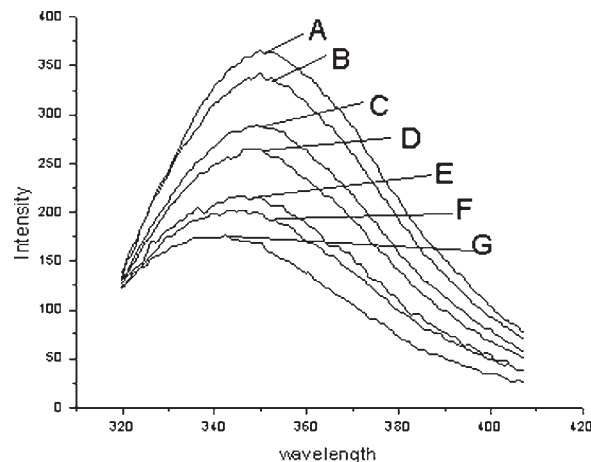


FIGURE 6 Emission spectra of $0.5 \times 10^{-6} \text{ mol dm}^{-3}$ BSA at pH 7 in the presence of TFE: 0 (A), 0.05 (B), 0.5 (C), 0.75 (D), 1.2 (E), 1.5 (F), and 3 (G) mol kg^{-1} .

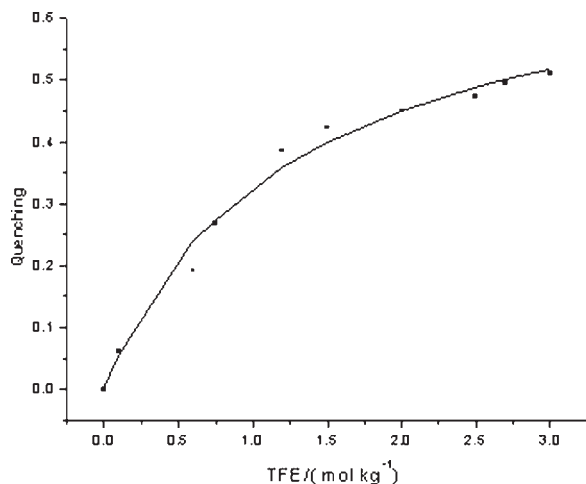


FIGURE 7 Quenching of $0.5 \times 10^{-6} \text{ mol dm}^{-3}$ of BSA at pH 7 and at different molalities of TFE.

the peptide and then providing a solvent matrix for further side-chain–side-chain interactions. It is also proposed that TFE may induce helicity by selectively raising the energy of solvent-exposed amide functionality in the coiled state.⁴⁴ Another model for indirect mechanism was reported in which the random coil was chosen as the most solvated state and hence most perturbed by the addition of cosolvent.⁴⁵ The helix formation is impeded by the entropic cost of assembling the aqueous solvent around the helix in pure water, and addition of TFE thus favors the helix as $d\Delta S/d[\text{TFE}] > 0$. Recently it has been proposed that TFE acts by selectively desolvating the peptide backbone groups of the helix and thereby inducing the helical state.⁴⁶ Based upon calorimetric, densimetric, and surface tension measurements, we have suggested that TFE–protein interaction⁴⁷ includes a combination of both solvent-mediated effects and direct binding. The ITC results in the present studies (Figures 8 and supplement 2) show that the heat liberated at each injection is nearly zero and the overall ITC profile does not indicate a significant binding pattern. These results do not indicate appreciable binding of TFE molecules to BSA, suggesting that the binding component to the overall interaction of TFE with the protein is very small and the solvent-mediated effects are dominant. The solvent-mediated effects may in turn affect the conformations of protein, which includes induction of helicity. The support for the dominant solvent-mediated effects also comes from the fact that the dielectric constant of TFE is about one-third of that of water,⁴⁸ which should lead to a strengthening of charge interactions including between partial charges as they occur in hydrogen bonds. TFE is also a weaker base and hence a much weaker hydrogen-bond acceptor and a

slightly stronger donor than water.⁴⁹ The bulky—CF₃ group also sterically hinders the interaction with the peptide backbone. These combined effects of strengthening hydrogen-bond interactions in the protein leads to an overall strengthening of intramolecular hydrogen bonds. Since the binding component is very weak, the anesthetic action of TFE molecules on the actual targets may be through the perturbation of the physical properties of the membrane.

CONCLUSIONS

TFE is observed to be a stabilizer or a destabilizer of the folded state of BSA depending on the pH. ITC results indicate an absence of appreciable binding of TFE to its native state as well as to its changed conformation at pH 9. DSC results also support the observations that TFE does not bind appreciably to BSA as no remarkable shift in thermal stability is seen. Addition of TFE to BSA

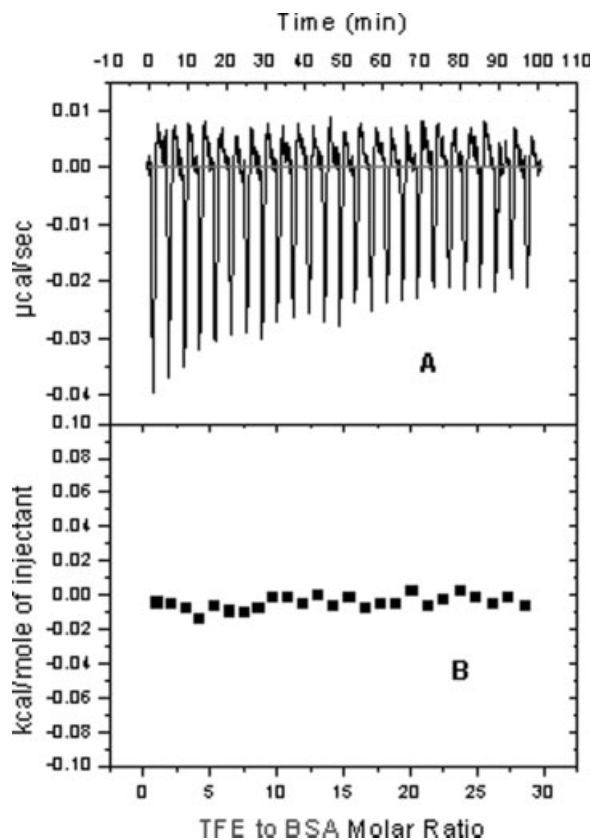


FIGURE 8 Titration of the $0.058 \times 10^{-3} \text{ mol dm}^{-3}$ BSA at pH 7 with $8.34 \times 10^{-3} \text{ mol kg}^{-1}$ TFE at 298.15 K, showing the calorimetric response as successive injections of ligand, are added to the reaction cell. Panel B depicts the isotherm of the calorimetric titration shown in panel A.

at pH 7 did not cause any change in tryptophan fluorescence at lower molalities and only at higher molalities some degree of quenching was observed, which could be due to solvent-mediated effects. A considerable lesser degree of quenching at pH 9 indicates that an increase in pH results in further weakening of hydrophobic interactions between tryptophan and TFE. The calorimetric and spectroscopic results obtained in this work suggest that the solvent-mediated effects dominate in the interaction TFE with BSA and that the binding component may be very weak. Since the binding component is very weak, one of the possibilities of anesthetic action of TFE molecules on the actual targets may be through perturbation of the structural and dynamic properties of the lipid bilayer so that the function of crucial but unspecified membrane proteins is affected.

This work was supported by funding from the Department of Science and Technology, New Delhi, India.

REFERENCES

1. Tanford, C. *Adv Protein Chem* 1968, 23, 121–282.
2. Lu, H.; Buck, M.; Radford, S. E.; Dobson, C. M. *J Mol Biol* 1997, 265, 112–117.
3. Chiti, F.; Taddei, N.; Webster, P.; Hamada, D.; Fiaschi, T.; Ramponi, G.; Dobson, C. M. *Nat Struct Biol* 1999, 6, 380–387.
4. Bychkova, V. E.; Dujsekina, A. E.; Klenin, S. I.; Ticktopulo, E. I.; Uversky, V. N.; Ptitsyn, O. B. *Biochemistry* 1996, 35, 6058–6063.
5. Cort, J.; Liu, Z.; Lee, G.; Harris, S. M.; Prickett, K. S.; Gaeta, L. S.; Anderson, N. H. *Biochem Biophys Res Commun* 1994, 204, 1088–1095.
6. Shiraki, K.; Nishikawa, K.; Goto, Y. *J Mol Biol* 1995, 245, 180–194.
7. Nelson, J.; Kallenbach, N. R. *Biochemistry* 1989, 28, 5256–5261.
8. Buck, M.; Schwalbe, H.; Dobson, C. M. *Biochemistry* 1995, 34, 13219–13232.
9. Hamada, D.; Kuroda, Y.; Tanaka, T.; Goto, Y. *J Mol Biol* 1995, 254, 737–746.
10. Kundu, A.; Kishore, N. *Biopolymers* 2004, 73, 405–420.
11. Mchaourab, H. S.; Hyde, J. S.; Feix, J. B. *Biochemistry* 1993, 32, 11895–11902.
12. Sirangelo, I.; Piaz, F. D.; Malmo, C.; Cassilo, M.; Birolo, L.; Pucci, P.; Marino, G.; Irace, G. *Biochemistry* 2003, 42, 312–319.
13. Hirota, N.; Mizuno, K.; Goto, Y. *Protein Sci* 1997, 6, 416–421.
14. Nelson, J. W.; Kallenbach, N. R. *Proteins* 1986, 1, 211–217.
15. Thomas, P. D.; Dill, K. A. *Protein Sci* 1993, 2, 2050–2065.
16. Dill, K. A.; Bromberg, S.; Yue, K.; Fiebig, K. M.; Yee, D. P.; Thomas, P. D.; Chan, H. S. *Protein Sci* 1995, 4, 561–602.
17. Liu, Y.; Bolen, D. W. *Biochemistry* 1995, 34, 12884–12891.
18. Shiraki, K.; Nishikawa, K.; Goto, Y. *J Mol Biol* 1995, 245, 180–194.
19. Synder, S. W.; Lador, U. S.; Wade, W. S.; Wang, G. T.; Barrett, Matayoshi, E. D.; Huffaker, H. J.; Krafft, G. A.; Holzman, T. F. *Biophys J* 1994, 67, 1216–1228.
20. Zhang, H.; Kaneko, K.; Nyugen, J. T.; Livshits, T. L.; Baldwin, M. A.; Cohen, F. E.; James, T. L.; Prusiner, S. B. *J Mol Biol* 1995, 250, 514–526.
21. Alexandrescu, A. T.; Ng, Y. L.; Dobson, C. M. *J Mol Biol* 1994, 235, 587–599.
22. Kumaran, S.; Roy, R. P. *J Pept Res* 1999, 53, 284–293.
23. Fujita, Y.; Miyanaga, A.; Noda, Y.; *Bull Chem Soc Jpn* 1979, 52, 3659–3662.
24. Schobrunner, N.; Wey, J.; Engels, J.; Georg, H.; Kiefhaber, T. *J Mol Biol* 1996, 260, 432–445.
25. Rajan, R.; Balaram, P. *Int J Pept Protein Res* 1996, 48, 328–336.
26. Jasanoff, A.; Fresht, A. R. *Biochemistry* 1994, 33, 2129–2135.
27. Luo, P.; Baldwin, R. L. *Biochemistry* 1997, 36, 8413–8421.
28. Krasowski, M. D.; Harrison, N. L. *Br J Pharmacol* 2000, 129(4), 731–743.
29. Kaminsky, L. S.; Fraser, J. M.; Seaman, M.; Dunbar, D. *Biochem Pharmacol* 1992, 44(9), 1829–1837.
30. Hansen, K. U. *Dan Med Bull* 1990, 37, 57–84.
31. Carter, D. C.; Ho, J. X. *Adv Protein Chem* 1994, 45, 152–203.
32. Peters, T. *All About Albumin: Biochemistry, Genetics, and Medical Applications*; Academic Press: San Diego, CA.
33. Peters, T., Jr. *Adv Protein Chem* 1985, 37, 161–245.
34. Kirchoff, W. H. EXAM, U.S. Department of Energy, Thermodynamics Division, National Institute of Standards and Technology, Gaithersburg, MD.
35. Yamasaki, M.; Yano, H.; Aoki, K. *Int J Biol Macromol* 1990, 12, 263–268.
36. Gerlisma, S. Y. *Eur J Biochem* 1970, 14, 150–153.
37. Fink, A. L.; Painter, B. *Biochemistry* 1987, 26, 1665–1671.
38. Chiou, J. S.; Ueda, I. *J Pharm Biomed Anal* 1994, 12, 969–975.
39. Jackson, M.; Mantsch, H. *Biochim Biophys Acta* 1992, 1118, 139–143.
40. Hong, D.; Hoshino, M.; Kuboi, R.; Goto, Y. *J Am Chem Soc* 1999, 121(37), 8427–8433.
41. Johansson, J. S. *J Biol Chem* 1997, 272, 17961–17965.

42. Johansson, J. S.; Eckenhoff, R. G.; Dutton, P. L. *Anesthesiology* 1995, 83, 316–324.
43. Reiersen, H.; Rees, A. R. *Protein Eng* 2000, 13(11), 739–743.
44. Goodwin, A. C.; Allen, T. J.; Oslick, S. L.; McClure, K. F.; Lee, J. H.; Kemp, D. S. *J Am Chem Soc* 1996, 118, 3082–3091.
45. Walgers, R.; Lee, T. C.; Goodwin, A. C. *J Am Chem Soc* 1998, 120, 5073–5079.
46. Starzyk, A.; Barber-Armstrong, W.; Sridharan, M.; Decatur, S. M. *Biochemistry* 2005, 44(1), 369–376.
47. Kundu, A.; Kishore, N. *Biophys Chem* 2004, 109, 427–442.
48. Llinas, M.; Klein, M. P. *J Am Chem Soc* 1975, 97, 4731–4737.
49. Nelson J., Kallenbach, N. R. *Proteins Struct Funct* 1986, 1, 211–217.

Reviewing Editor: David E. Wemmer